

Supplement of Atmos. Chem. Phys., 16, 14635–14656, 2016  
<http://www.atmos-chem-phys.net/16/14635/2016/>  
doi:10.5194/acp-16-14635-2016-supplement  
© Author(s) 2016. CC Attribution 3.0 License.



Atmospheric  
Chemistry  
and Physics  
Open Access  
EGU

*Supplement of*

## **Effect of vehicular traffic, remote sources and new particle formation on the activation properties of cloud condensation nuclei in the megacity of São Paulo, Brazil**

**Carlos Eduardo Souto-Oliveira et al.**

*Correspondence to:* Carlos Eduardo Souto-Oliveira ([carlos.edu.oliveira@usp.br](mailto:carlos.edu.oliveira@usp.br))

The copyright of individual parts of the supplement might differ from the CC-BY 3.0 licence.

## Supplementary Information (SI)

**Table S1.** Detailed information related to the Fig. 1. In this table are described the instrumental and local conditions, as well as regions and values.

Country	Sites	year / period	id	PCN $\pm$ SD ( $\times 10^6$ cm <sup>-3</sup> )	CCN (65%) ( $\times 10^3$ cm <sup>-3</sup> )	Instrument	vehicle (million)	inhabitant (million)	Populational density (km <sup>-2</sup> )	Sampling site	Reference	
Brazil	São Paulo	2014 (Aug/Sep) 14 days	1.1 CCN and PCN mean	11.6 $\pm$ 3.1	2(0.2), 2.6(0.4), 3.2(0.6), 3.6(0.8), 4(1.0)	DMT CCN-100 (SS.0.2 - 1.0%)	7	20	2552.0	Roof top of building (30m above ground) urban area	This study	
			1.2 Diurnal mean	16.4 $\pm$ 7.9	1.7(0.2), 2.5(0.4), 3.2(0.6), 3.6(0.8), 4(1.0)	DMPS (10-450 nm)						
			1.3 Nocturnal mean	6.9 $\pm$ 3.4	1.7(0.2), 2.7(0.4), 3.3(0.6), 3.7(0.9), 4(1.0)	DMPS (10-450 nm)						
	São Paulo	2012 (Oct - 15 days)	2 CCN and PCN mean	12.8 $\pm$ 5.4	1.1(0.2), 2.2(0.5), 2.8(0.7), 3.2(0.9), 3.6(1.1)	DMT CCN-100 (SS.0.2 - 1.0%)	7	20	-	Roof top of building (40m above ground) urban area	Ameida et al., 2014	
	São Paulo	2010 Oct - 2011 Jan (79 days)	3 PCN mean	23.5	-	DMPS (6 - 800 nm)	7	20	-	Roof top of building near urban area	Backman et al., 2012	
China	Shanghai	2010 - 2011 (1 Year)	4 CCN and PCN continental air mean	10	4.5(0.2), 5.7(0.4), 7(0.6), 7.8(0.8), 8.2(1.0)	DMT CCN-100 (SS.0.07 - 2%)	2.2	24	3800	Roof top of building (30m above ground) residential urban area	Leng et al., 2013	
			5 PCN mean	12.9	-	DMPS (15-600 nm)	2.2	24	-	-	Roof six-floor building, urban residential and business areas	Peng et al., 2014
	Beijing	2008 (Aug/Sep)	6.1 CCN and PCN mean 6.2 Fresh city pollution 6.3 Aged regional pollution	16.5 $\pm$ 9.0 22.5 $\pm$ 7.3 11.9 $\pm$ 2.8	5.7(0.26), 7.7(0.46), 8.7(0.66), 8.9(0.86) 2.9(0.26), 5.0(0.46), 6.8(0.66), 8.3(0.86) 7.3(0.26), 8.8(0.46), 9.2(0.66), 9.9(0.86)	DMT CCN-100 (SS.0.07 - 0.65%)	2.6	18.6	1300	Roof top third-floor building in a suburban area	Gunther et al., 2011	
Mexico	Mexico City	2006 (Mar)	7 PCN mean	21	-	DMPS (15 - 494 nm)	4	20	6000	Residential and light industrial area	Kalaliu-Petibone et al., 2011	
Spain	Madrid	2007-2008	8 PCN mean	9.9	-	DMPS (15 - 1000 nm)	4	6	5325	Park inside metropolitan region	Gómez-Moreno et al., 2011	
UK	London	2009	9 PCN mean	12.1 $\pm$ 5.8	-	DMPS (7 - 1000 nm)	2.6	13	5223	North Kensington, surrounded by a mainly residential area.	Reche et al., 2011	

Reference	Site	Environment	0.20%	0.40%	0.60%	0.80%	1.0%	
<b>This study</b>	<b>Total mean</b>		136±43	108±36	91±35	81±34	74±34	
	<b>Diurnal</b>	Sao Paulo	Urban	155±46	127±32	110±29	99±29	92±29
	<b>Nocturnal</b>			115±25	87±28	71±28	61±28	54±28
<b>Leng et al.(2013)</b>	Shanghai	Urban/Coast	-	-	-	41 <sup>a</sup> - 68 <sup>b</sup>	-	
<b>Burkart et al.(2011)</b>	Vienna	Urban	-	-	69 - 368 <sup>c</sup>	-	-	
<b>Sihito et al.(2011)</b>	Finland	Forest	-	58 - 99	-	-	-	
		Coast	-	70 - 90 <sup>d</sup>	-	-	-	
<b>Quinn et al.(2008)</b>	Gulf of Mexico	Urban	-	> 90 <sup>e</sup>	-	-	-	
	Atlantic Ocean	Over Ocean	-	< 80	-	-	-	
<b>Furutani et al.(2008)</b>	California	Urban/Coast	-	-	70 - 110 <sup>d</sup>	-	-	
			-	-	~110 <sup>f</sup>	-	-	
	Pacific Ocean	Over Ocean	-	-	50 - 60	-	-	

a - Marine air

b - Continental air

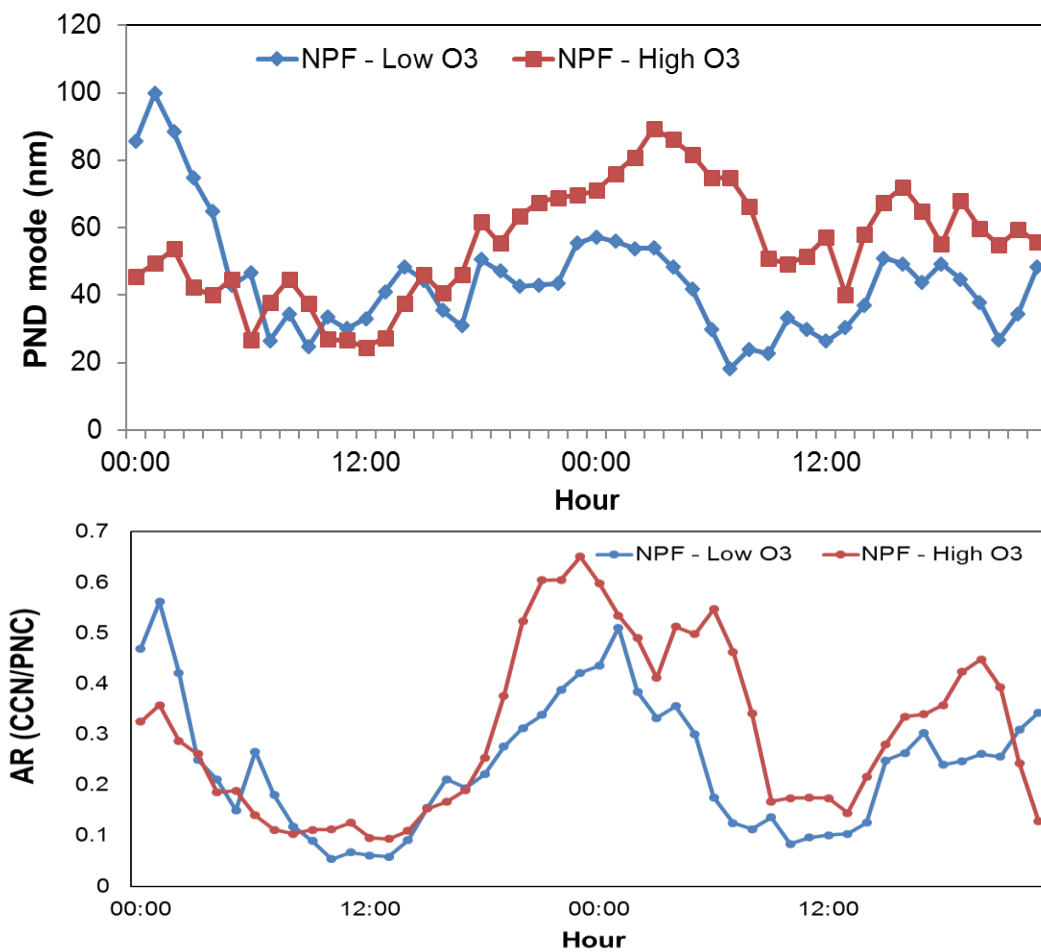
c - min-max at SS = 0.5%

d - Anthropogenic emissions or polluted air masses

e - Urban and industrial sources

f - Fresh Ship Exhaust

**Table S2.** Comparison between  $D_{act}$  calculated in this study and those reported in previous studies. These activation diameters were calculated using the same principle.



5

**Figure S1.** Hourly mode of particle diameter (PND mode) and AR (SS 0.4%) for NPF events with low and high O<sub>3</sub> concentrations. In order to evaluate particle increase were plotted the day after NPF event. The days after NPF-low O<sub>3</sub> showed low O<sub>3</sub> concentrations also, which can explain the lower diameter and AR for these days compared with days after NPF-high O<sub>3</sub>.

10

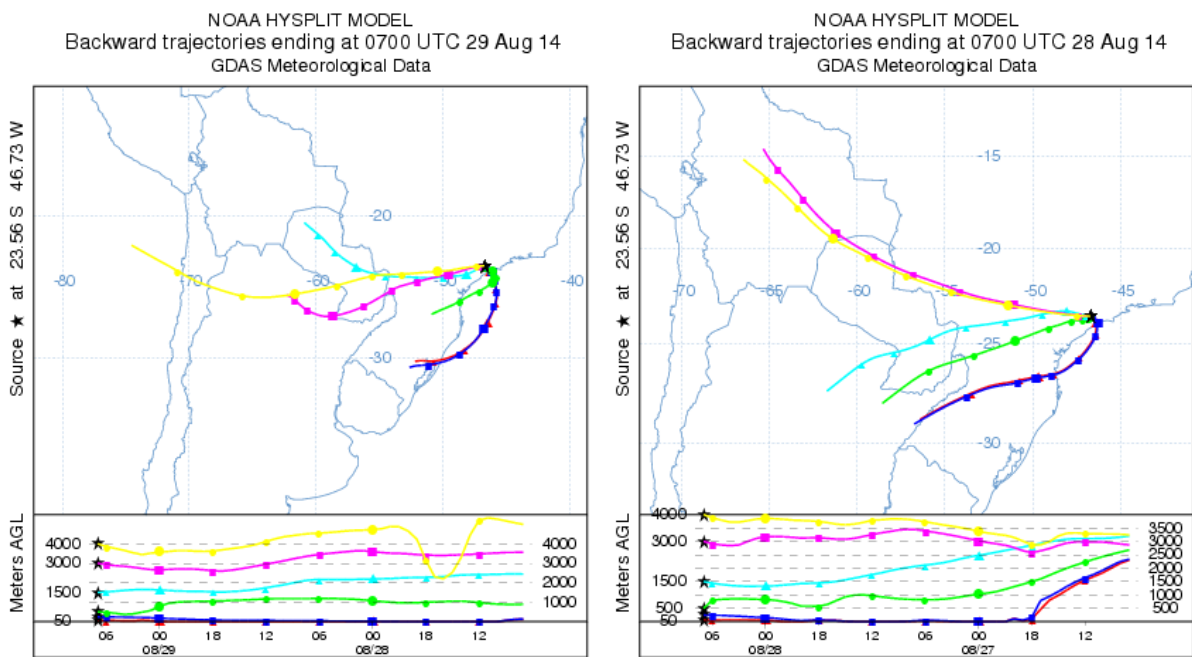
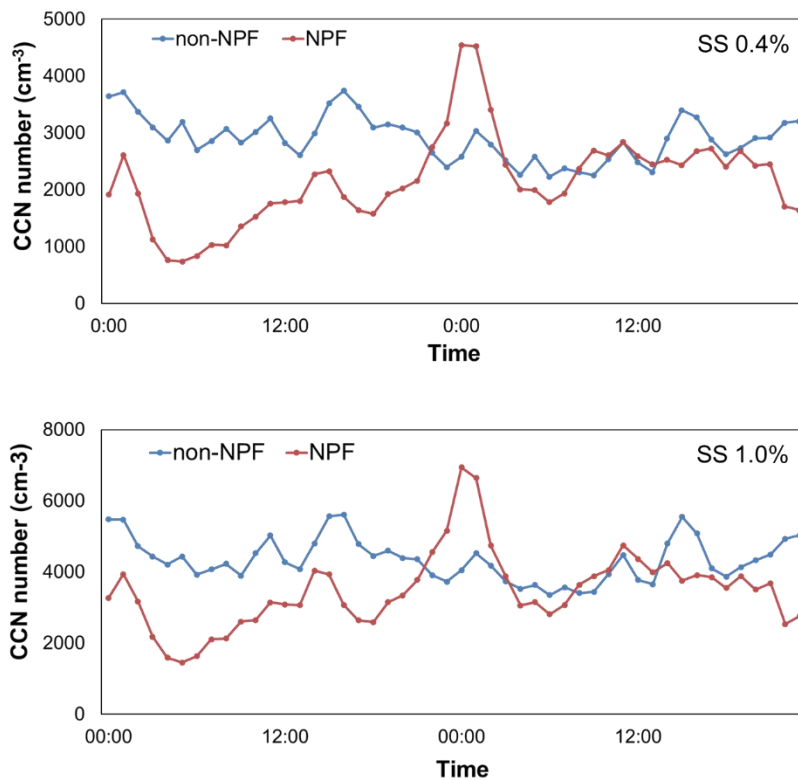


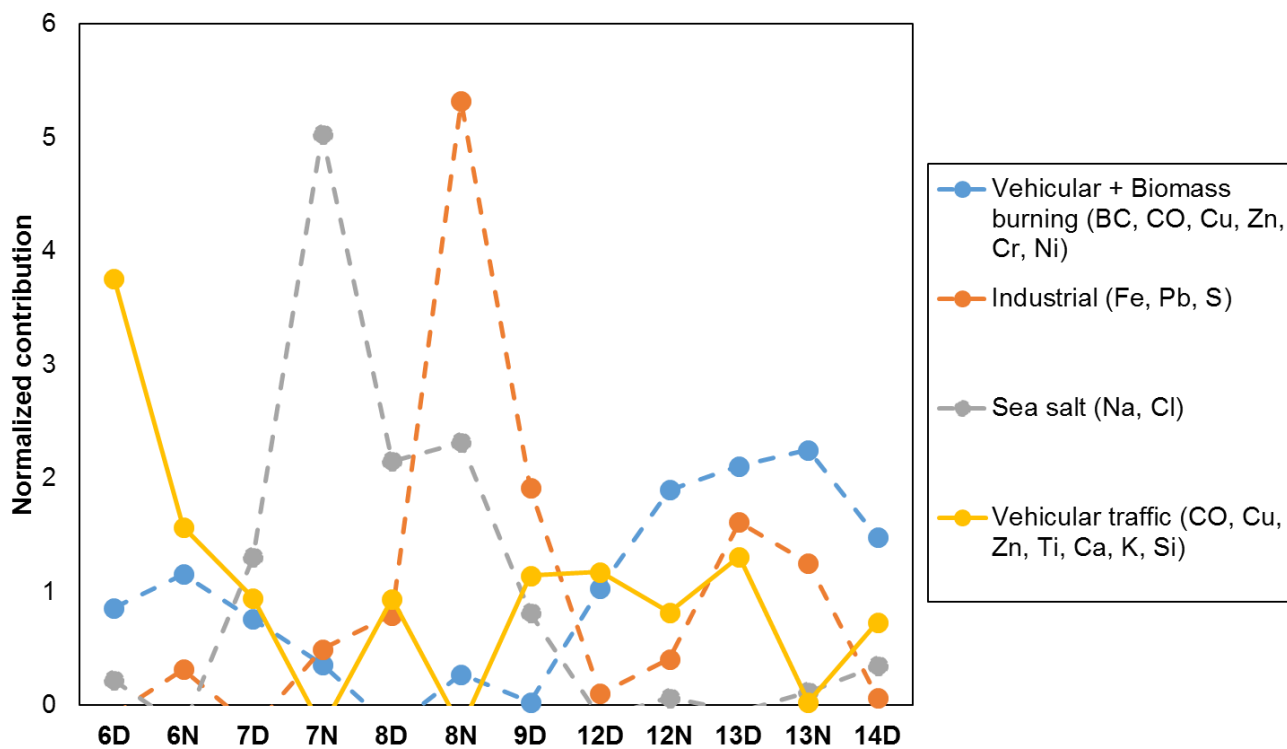
**Figure S2.** Hysplit backward trajectories models for days 7 and 8. For these period was observed Cl and Pb higher concentrations which were associated with air masses from ocean, as discusses in Section 3.3.



10

**Figure S3.** CCN number concentrations during NPF and non-NPF days. CCN averages were calculated for 48h period, being the first day select as NPF or non-NPF, while the second day was not considered in this classification. During NPF days the CCN number is lower than non-NPF days in agreement with previous discussion about AR showed in Fig. 8. In this figure can be seen clearly the enhancement of CCN number for NPF days in comparison with non-NPF.

15



5

**Figure S4.** Source apportionment analysis performed by positive matrix factorization (PMF) model, using elemental, carbon monoxide and BC concentrations. Vehicular traffic showed major contributions in most days during daytime mainly, whereas vehicular + biomass burning had main contributions on days 6, 12 and 13. Sea salt and industrial apportionment was most pronounced during days 7 and 8.

15

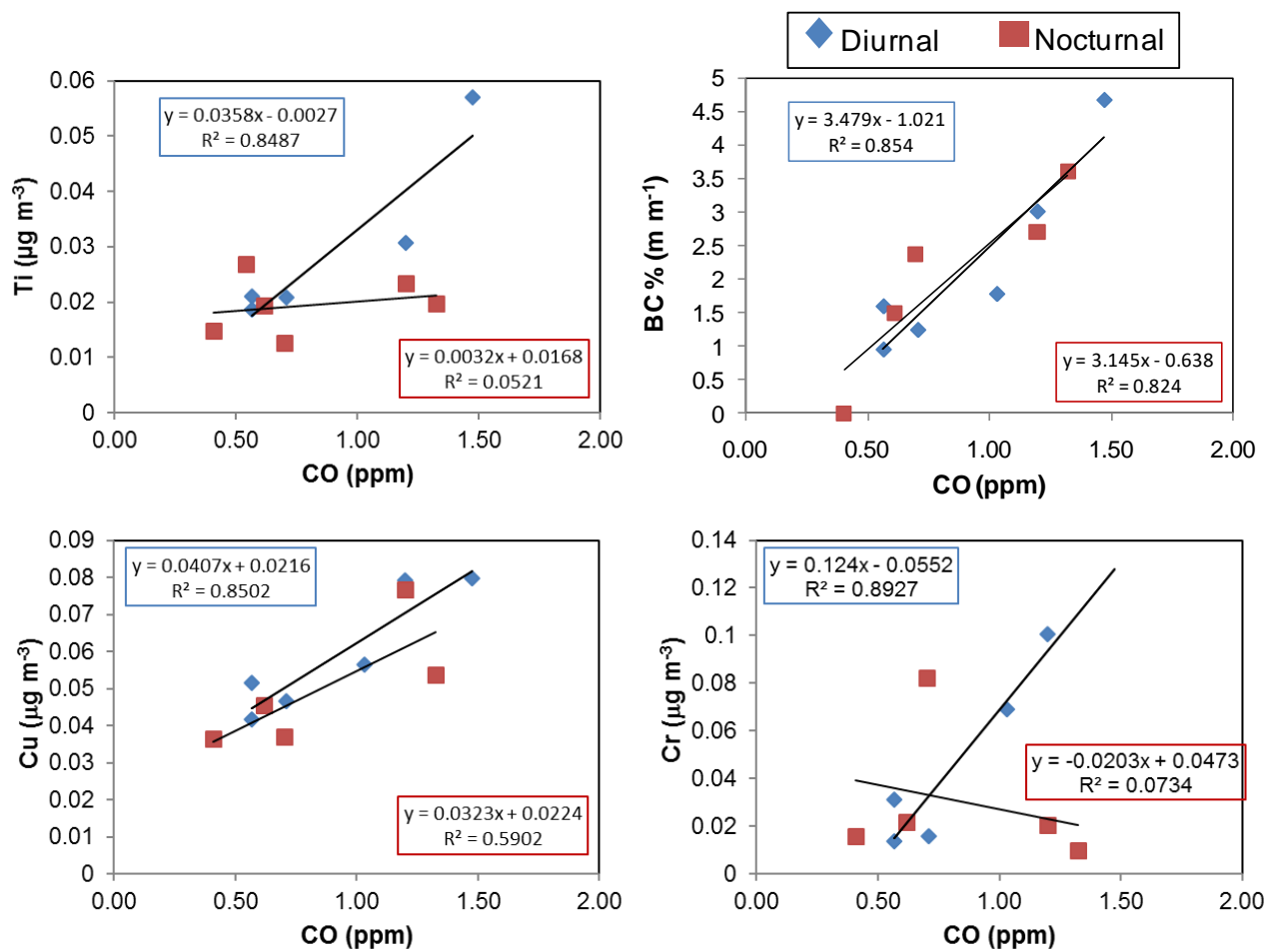


**Figure S5.** Elemental and BC concentrations versus carbon monoxide (CO). The strong correlation between vehicular markers species and CO during daytime confirm the major apportionment of this source to aerosol for all days. The strong correlation between BC, Cu and CO during nighttime can be related vehicular + biomass burning events.



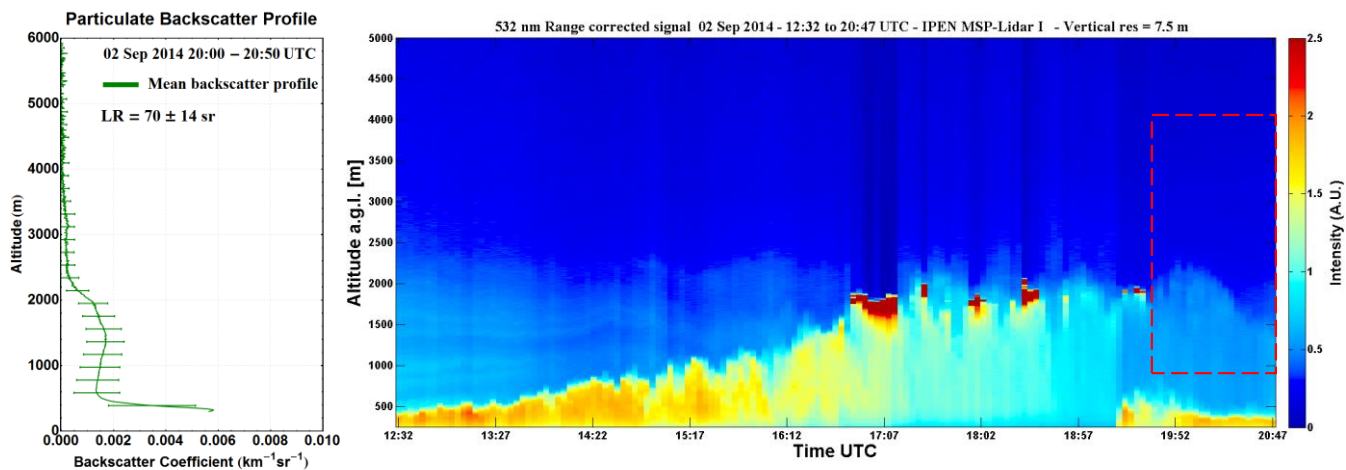


**Figure S6.** The particulate backscatter profile and lidar analyses for day13, when the prevailing wind was from the north or north-east, where most biomass burning events occur. The biomass burning plumes were detected by lidar and Geostationary Operational Environmental Satellite.